Source time functions of earthquakes based on a stochastic differential equation

Shiro Hirano[1]

[1]Department of Physical Science, College of Science and Engineering, Ritsumeikan University, 1-1-1, Nojihigashi, Kusatsu, Shiga, 525-8577, Japan

Key Points:

- Earthquake source time functions are modeled by the convolution of two solutions of a stochastic differential equation.
- Modeled functions are dominantly unimodal, evolve as $\sim t^3$, have ω^{-2}-like spectra, and satisfy the Gutenberg-Richter law.
- This convolution may mean that both the stress drop rate and fault impedance can be modeled as Bessel processes.

Corresponding author: Shiro Hirano, s-hrn@fc.ritsumei.ac.jp

Abstract

Source time functions are essential observable quantities in seismology; they have been investigated via kinematic inversion analyses and compiled into databases. Given the numerous available results, some empirical laws on source time functions have been established, even though they are complicated and fluctuate along time series. Theoretically, stochastic differential equations, which include a random variable and white noise, are suitable for modeling such complicated phenomena. In this study, we model source time functions as the convolution of two stochastic processes (known as Bessel processes). We mathematically and numerically demonstrate that this convolution satisfies some of the empirical laws of source time functions, including non-negativity, finite duration, unimodality, a growth rate proportional to t^3, ω^{-2}-type spectra, and frequency distribution. We interpret this convolution and speculate that the stress drop rate and fault impedance follow the same Bessel process.

Plain Language Summary

Earthquakes are high-speed slips of two rock masses that are followed by seismic wave radiation; it is important to quantify the time series of the slip rate during an earthquake. Many studies have revealed some empirical laws on the slip rate via time-series, Fourier, and statistical analyses, while they appear to be complicated, fluctuating, and individual. Using mathematical and numerical analyses, we reproduce these empirical laws using the theory of stochastic random processes. We also speculate on the physical reasoning as to why the mathematical model works well. Our theory may explain why earthquakes are complex and diverse.

1 Introduction

Earthquake source time functions (STFs), which are temporal variations in the slip rate integrated over faults during earthquakes, are macroscopically observable in seismology and have been widely investigated regarding kinematic source inversions and dynamic source modeling. To review some knowledge on STFs, we first summarize some empirical laws (ELs) for STFs:

EL1 STFs are dominantly non-negative, continuous, compactly supported, and unimodal.
EL2 The moment functions, which are proportional to the time-integration of STFs, evolve as $\sim t^3$, where t is the time since their ignition (this is referred to as "the cube law" herein).
EL3 The ω^{-2}-model can satisfactorily approximate the amplitude of STF Fourier spectra.
EL4 The frequency of their total moment follows the Gutenberg-Richter (GR) law.

Many studies, from early pioneering research (e.g., Houston, 2001) to recent revelations (e.g., Yin et al., 2021) have cataloged numerous STFs and revealed their tendencies and variabilities over time. Although several outliers have been found, EL1 has arisen as an obvious tendency, based on cataloged data. For example, ∼80% of the cataloged STFs are unimodal; they are labeled Group 1 in the research of Yin et al. (2021). In EL1, the fact that STFs are compactly supported is natural because regular earthquakes terminate within a few minutes, whereas slow earthquakes have longer durations.

Uchide and Ide (2010) compared the moment functions of $M_\mathrm{w}1.7-6.0$ events in Parkfield, California, based on multi-scale inversion analyses. They pointed out that EL2 holds from the very early to later stages of the source processes. Meier et al. (2016) demonstrated that peak ground displacement evolves with the cube law. As the far-field ground displacement is proportional to STFs, they suggested that the law is sourced from the phenomenon of self-similar rupturing of the fault, which results in EL2. In addition, the proportionality between the final moment and the cube of the total duration has been established (e.g., Houston, 2001).

Given the spectra of STFs, their amplitudes above their corner frequencies can be modeled by a power law, and their fall-off rates can be quantified. As shown by numerous studies (e.g., Boatwright, 1980; Abercrombie, 1995; Kanamori, 2014), EL3 seems to be very robust. Some forward modeling studies of dynamic rupturing have been conducted to explain the ω^{-2}-model; they have shown that STFs consist of functions that are almost entirely smooth, except for a kink. For example, Brune's model has a kink at its start, while Sato & Hirasawa's model and Madariaga's model both have a kink due to their stopping phases (see the review of Madariaga & Ruiz, 2016, on each mathematical or numerical representation). However, the cataloged STFs do not show such an isolated kink, but do show some fluctuations (Yin et al., 2021). This implies that the traditional modeling approaches are too simplified to reproduce the complexity of STFs, and thus, that some stochastic modeling is required.

Apart from the entire shape of each STF as discussed above, it has been well established that EL4 holds. The GR law originally means that the probability density function (PDF) of a seismic moment is a power law. By recalling the cube law between the moment and the duration, the GR law means that the PDF of the duration is also a power law. Once we model stochastic STFs, we can estimate the PDF of the duration and discuss whether the PDF satisfies the GR law.

The stochastic modeling of faulting processes has been proposed both theoretically and numerically. Andrews (1980, 1981) considered a spatio-temporal slip distribution with self-affinity, mainly in the Fourier domain. This approach revealed the spectra of the distribution and energetics of the faulting. Significantly, the fault impedance, which is the factor of proportionality between the slip rate and stress drop in the Fourier domain, can enlighten the relationship between the quantities, even in the stochastic model. After Andrews (1980, 1981), the importance of stochasticity has been more recognized (see the introduction of Aso et al. (2019) for details). Aso et al. (2019) introduced temporal stochasticity into their boundary integral equation for the dynamic rupture process and demonstrated the rupture complexity. While such numerical modeling is developing, mathematical modeling, if available, would contribute to the understanding of complex faulting processes.

Stochastic differential equation(SDE)-based models have been employed in the field of earthquake source physics. Matthews et al. (2002) and Ide (2008) modeled recurrent and slow earthquakes, respectively, as Brownian motion. Matthews et al. (2002) focused on regular earthquakes; however, the time scale considered by them was longer than each event, and they did not consider the properties of STFs. Wu et al. (2019) assumed that the generalized Langevin equation can model the equation of motion for the fault slip rate. Although their model was based on some physical properties of dynamic friction, their solution was Brownian motion, which cannot satisfy the non-negativeness (EL1) or the ω^{-2}-like spectrum (EL3). Thus, a novel approach is need for SDE-based modeling under EL1–4.

In this article, we consider an SDE known as the Bessel process. We analytically and numerically demonstrate that the convolution of two solutions from the same Bessel process satisfies EL1–4. Finally, we discuss the physical meaning of these two solutions on the basis of the fault impedance.

2 Mathematical modeling

In the following, we do not distinguish STF $:= \int_\Gamma V(\boldsymbol{x},t)\,d\boldsymbol{x}$ and moment-rate function $\dot{M}(t) := \mu \int_\Gamma V(\boldsymbol{x},t)\,d\boldsymbol{x}$ on a flat fault Γ, where μ is the rigidity and V is the slip rate distribution. We introduce a mathematical model to generate $\dot{M}(t)$ using solutions of an SDE. Ide (2008) modeled $\dot{M}$ for slow earthquakes as Brownian motion because the observed source spectra of slow earthquakes follow the ω^{-1}-model, which is similar to the spectrum of Brownian motion. For regular earthquakes, however, EL3 holds. Thus, we consider a product of the spectra of two stochastic processes (i.e., $\omega^{-1} \times \omega^{-1} = \omega^{-2}$), which is a convolution of the two stochastic processes in the time domain, which we denote as $X_t^{(1)}$ and $X_t^{(2)}$ herein. Thus, we assume that $\dot{M} = X_t^{(1)} * X_t^{(2)}$ holds, where the asterisk "*" denotes the convolution in time.

To fulfill EL1, we assume that both $X_t^{(1)}$ and $X_t^{(2)}$ are solutions of the following SDE called the Bessel process:

$$dX_t^{(i)} = \frac{d-1}{2}\frac{dt}{X_t^{(i)}} + dB_t^{(i)}, \quad (i = 1, 2) \tag{1}$$

with its initial value $X_0^{(i)}$ (> 0), which is equivalent to the integral form as:

$$X_t^{(i)} = X_0^{(i)} + B_t^{(i)} + \frac{d-1}{2}\int_0^t \frac{ds}{X_s^{(i)}}, \quad (i = 1, 2) \tag{2}$$

where $B_t^{(i)}$ is a standard Brownian motion and d is the dimension of the Bessel process. SDE(1) is valid while $X_t^{(i)} > 0$ holds. Thus, we define $X_t^{(i)} = 0$ after the process hits zero; the time $T := \min_t \left\{ t | t > 0 \,\&\, X_t^{(i)} = 0 \right\}$ is referred to herein as the first hitting time (Göing-Jaeschke & Yor, 2003). According to the above definition, $X_t^{(i)}$ is continuous and non-negative. Moreover, $X_t^{(i)}$ with $d < 2$ is compactly supported because $T \ll \infty$ holds almost surely if $d < 2$ (Göing-Jaeschke & Yor, 2003). Therefore, given $d < 2$, EL1 holds if we can confirm that $X_t^{(1)} * X_t^{(2)}$ is unimodal. We demonstrate this statement numerically in the next section.

We also confirm that $X_t^{(1)} * X_t^{(2)}$ satisfies EL2 and EL3 numerically in the next section. It can be expected that EL3 would be satisfied, as described in the first paragraph of this section.

The condition for EL4 can be derived analytically. Hamana and Matsumoto (2013) showed that $P(T)$, which is the PDF of the first hitting time T with $d < 2$ and $X_0^{(i)} = a$, can be represented as:

$$P(T) = \frac{2^\nu}{a^2\Gamma(|\nu|)} T^{\nu-1} \exp\left(-\frac{a^2}{2T}\right), \tag{3}$$

where $\nu = \frac{d}{2} - 1$, and $\Gamma(\cdot)$ is a gamma function. On the other hand, considering the cube law ($M_0 \sim T^3$), the GR law with respect to $M_w = \frac{2}{3}\log_{10} M_0 - 6.1$ can be represented as

$$P(M_w) \sim 10^{-bM_w} \sim T^{-2b}, \tag{4}$$

where $b \sim 1$ holds and the constant coefficients are neglected. Thus, if we assume a sufficiently small initial value, $a\,(\ll \sqrt{2T})$, eqs (3) and (4) imply that:

$$\nu = -2b + 1, \quad \text{i.e.,} \quad d = 4(1 - b) \tag{5}$$

is required for EL4.

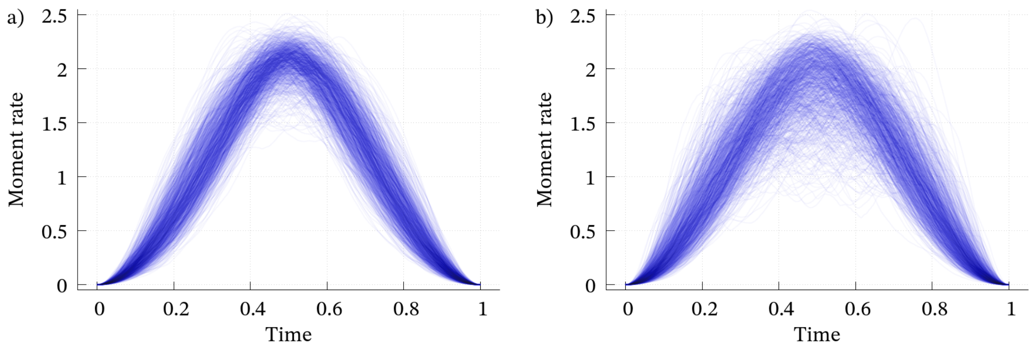

Figure 1. The 1,000 computed convolutions of the two Bessel processes for (a) case A and (b) case B. Time scale and total moment are normalized.

3 Numerical Modeling and Results

In the following section, we investigate how the convolution $X_t^{(1)} * X_t^{(2)}$ satisfies EL1–3 after solving eq.(1) using the SRIW1 algorithm (Rößler, 2010) implemented in DifferentialEquations.jl (https://diffeq.sciml.ai/) for Julia 1.6.1 (https://julialang.org/). Given eq.(5) and $b = 1$, we solve:

$$dX_t = -\frac{1}{2}\frac{dt}{X_t} + dB_t$$

with a constant time step of $dt = 10^{-6}$ and a sufficiently small initial value of $X_0 = 10^{-3}$ up to time $T_{\max} = 2{\times}10^{-3}$ (i.e., 2,000 steps). Because the solution must become zero in our model, we reject numerical solutions that never reached zero before $T_{\max}$. The convolution of two solutions does not follow ω^{-2}-model if their corner frequencies, which are comparable to the inverse of their fist hitting time, are quite different. Thus, we denote the lower limit of the first hitting time as $T_{\min}$ and reject solutions that reach zero before $T_{\min}$. In the following, we investigate two cases: A) $T_{\min} = 2 \times 10^{-4}$ (i.e., 200 steps) and B) $T_{\min} = 1 \times 10^{-3}$ (i.e., 1,000 steps). Therefore, we consider the Bessel processes with the probabilistic first hitting time T satisfying $T_{\min} \leq T \leq T_{\max}$, where $T_{\min}/T_{\max} = 0.1$ for case A and $T_{\min}/T_{\max} = 0.5$ for case B. For every two solutions, we regard the solution with relatively shorter duration as $X_t^{(1)}$ and the other as $X_t^{(2)}$. Thus, $T_{\min}/T_{\max} \leq T_1/T_2 \leq 1$ holds, where T_i is the duration for $X_t^{(i)}$ $(i = 1, 2)$.

After iterations, we store 2,000 solutions with $T_{\min} \leq T \leq T_{\max}$, which yields 1,000 pairs of solutions, and calculate 1,000 convolutions of the pairs. Even though we calculate and abandon many useless solutions, we obtain ∼120 Bessel processes per minute within the duration range by using 12-core AMD Ryzen 9 3900XT.

The 1,000 convolutions dominantly satisfy EL1 (Fig.1), whereas the case B shows more variation (see Supporting Figures for individual cases). Simultaneously, the time integration (Fig.2) and Fourier amplitude spectra (Fig.3) reproduce EL2 and EL3, respectively. EL4 is almost surely satisfied, as discussed in the previous section. Hence, we conclude that the convolution of two Bessel processes with $d = 0$ stochastically fulfills EL1–EL4.

4 Discussion

Here, we interpret the physical meaning of the convolution of two Bessel processes. In the following, we consider a finite flat fault surface Γ and define two convolutions: "$*$" as only in time and "$\tilde{*}$" as in on-fault position and time. In the case of a finite fault, we

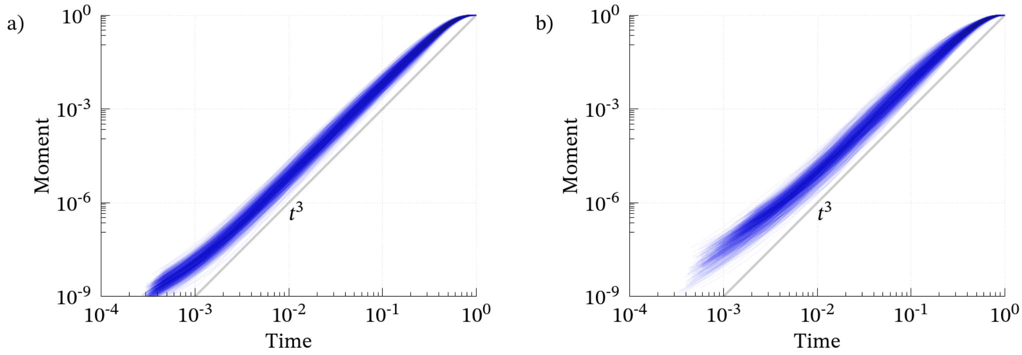

Figure 2. The normalized moment evolution $\left(\int_0^t \dot{M}(s)\,ds / \int_0^\infty \dot{M}(s)\,ds\right)$ for (a) case A and (b) case B along normalized time scale (t/T). The curves dominantly follow the cube law ($\sim t^3$) except for in their initial stages, which are affected by their initial values, and in their final stages, which converge toward their static states.

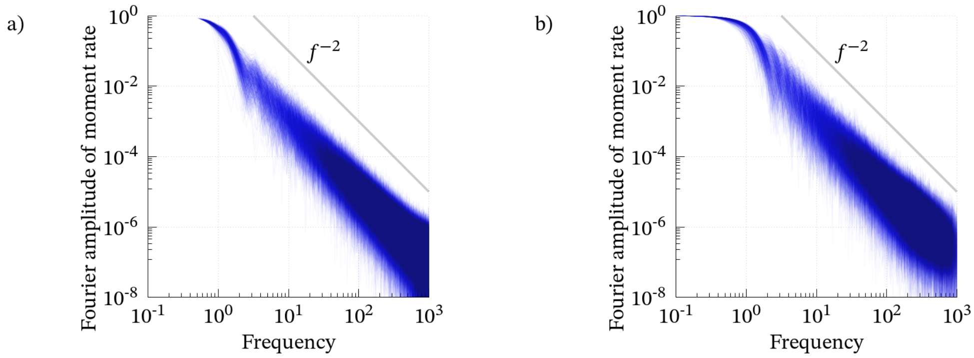

Figure 3. The normalized Fourier amplitude spectra of the convolutions plotted in Fig.1 for (a) case A and (b) case B.

assume that the stress drop rate, $\dot{\sigma}(\boldsymbol{x},t)$ for the on-fault position $\boldsymbol{x} \in \Gamma$, can be represented as:

$$\dot{\sigma}(\boldsymbol{x},t) = -\left(\dot{m}\tilde{*}Z\right)(\boldsymbol{x},t), \tag{6}$$

where $\dot{m}(\boldsymbol{x},t)$ is the moment-rate density function and $Z(\boldsymbol{x},t)$ is the fault impedance, as detailed by Andrews (1980, 1981). If the surrounding area is an elastic body, Z can be derived from linear elasticity. However, we consider a stochastic process in which Z includes a non-deterministic property. Eq.(6) represents the stress rate (i.e., Neumann condition) based on the displacement discontinuity (i.e., Dirichlet condition) along a finite fault; thus, Z is called a Dirichlet-to-Neumann operator. Here, we assume that there exists a Neumann-to-Dirichlet operator Z^{-1}, whose support is Γ, satisfying:

$$\dot{m}(\boldsymbol{x},t) = -\left(\dot{\sigma}\tilde{*}Z^{-1}\right)(\boldsymbol{x},t). \tag{7}$$

Furthermode, the Fourier transform with respect to position ($\int_\Gamma e^{2\pi i \boldsymbol{k}\cdot\boldsymbol{x}} d\boldsymbol{x}$, where $\boldsymbol{k}$ is a two dimensional wavenumber) yields:

$$\dot{m}(\boldsymbol{k},t) = -\left(\dot{\sigma}(\boldsymbol{k},\cdot) * Z^{-1}(\boldsymbol{k},\cdot)\right)(t). \tag{8}$$

As the limit $\boldsymbol{k} \to 0$ is equivalent to the integration in space ($\lim_{\boldsymbol{k}\to 0} \int_\Gamma e^{2\pi i \boldsymbol{k}\cdot\boldsymbol{x}} d\boldsymbol{x} = \int_\Gamma d\boldsymbol{x}$), eq.(8) results in

$$\overline{\dot{m}}(t) = \dot{M}(t) = -\left(\overline{\dot{\sigma}} * \overline{K^{-1}}\right)(t), \tag{9}$$

where the overlines denote integration over Γ. Finally, eq.(9) implies that EL1–4 are fulfilled if the stress rate, $\overline{\dot{\sigma}}(t)$, and Neumann-to-Dirichlet operator, $\overline{Z^{-1}}$, when integrated over Γ, are Bessel processes.

As σ comprises stress *drop*, $-\overline{\dot{\sigma}}(t)$ is always non-negative and $-\overline{\sigma}(t)$ is a non-decreasing function from zero to its final value (> 0). This property is naturally produced if $-\overline{\dot{\sigma}}(t)$ is a Bessel process. For the 1,000 results, $X_t^{(1)} * X_t^{(2)}$, as obtained in the previous section, we also calculate $-\int_0^t X_s^{(1)}\, ds$, where the duration of $X_s^{(1)}$ is shorter than that of $X_s^{(2)}$. By considering this quantity as $\overline{\sigma}(t)$, we confirm the relationship between $M(t)$ and $\overline{\sigma}(t)$. The results show monotonic slip-weakening curves (Fig.4). Therefore, the assumption that the stress drop rate is a Bessel process explains the natural weakening process of the on-fault stress change. In Fig.4, the abscissa and ordinate mimic averaged slip and stress drop over the fault, respectively. This means that the characteristic slip weakening distance ranges from 20% to 50% of the final slip amount. Interestingly, this fraction is close to results obtained based on observations (e.g., Mikumo, 2003).

To interpret the other assumption that the inverse fault impedance, $\overline{Z^{-1}}$, is a random process is not straightforward. When we calculate seismic waves, the Green functions are well modeled within the framework of linear elasticity. This might be because the Green functions depend on the medium between the fault and (usually) far-field observation points, where almost all of the region is an elastic body. However, the (inverse) fault impedance is a propagator among the on-fault positions traveling along the fault. In general, faults are segmented, bumpy, and surrounded by fractured rocks. Modeling such a complex system by assuming a flat fault may cause non-deterministic fluctuations due to scattering waves, as schematically illustrated by Aso et al. (2019). Therefore, this assumption is possible, even though it is difficult to directly observe.

In the numerical simulation, we restrict the ratio of the duration of $X_t^{(1)}$ and $X_t^{(2)}$ within tenfold. This is not only for EL3, as mentioned here, but also for another physical property. If $X_t^{(1)}$ is the stress drop rate, its duration should correspond to the duration of the most energetic faulting process, which is given by the fault length divided

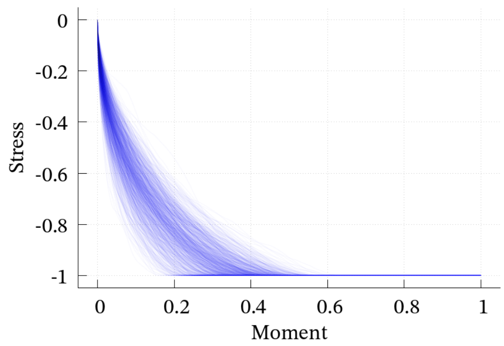

Figure 4. Normalized moment versus normalized stress drop assumed to be time-integration of a Bessel process for case A.

by the rupture speed. On the other hand, because $\overline{Z^{-1}}(t) = X_t^{(2)}$ is based on the fault impedance, its duration must be equivalent to the time taken for the scattering wave to spread over the entire fault. This time is at least, or even a few times greater than, the fault length divided by the seismic wave speed. Therefore, the durations of $X_t^{(1)}$ and $X_t^{(2)}$ should have almost the same order, and $T_{\min}/T_{\max} = 0.1$ and 0.5 in our assumption might be two possible end members.

5 Conclusions and outlooks

Here we demonstrate that the four empirical laws on STFs, or moment-rate functions, can be reproduced by modeling STFs as the convolution of two Bessel processes with almost the same order of duration. In terms of fault mechanics, given the complexity of the geometry and surroundings of the faults, this result is comprehensible if both the stress drop rate and the inverse fault impedance follow a Bessel process.

One possible future approach could be to extend the model by considering spatial heterogeneity of stress, fault geometry, and the surrounding medium. This is similar to the numerical model of Aso et al. (2019); further mathematical model and results will broaden our understanding. The main difficulty might be that we must somehow consider a stochastic partial differential equation that considers both space and time, which is a more mathematically challenging task. Were such a model available, it would be possible to discuss the physical processes related to rupture initiation, propagation, and termination as stochastic processes. Moreover, some relationships between the kinetic and potential energies released from heterogeneous slip distribution (e.g., Hirano & Yagi, 2017) could be revealed, which would be necessary for the energetics of faulting.

A future plan could be to apply our model to scientific and engineering studies on strong ground motions. One way to numerically simulate strong ground motions is to compute the convolution of an STF and the Green function. However, this STF should not be unique, even if we consider a single fault, and stochastic simulation would be required by assuming various STFs. Our model allows us to generate numerous STFs using a the stochastic process that leads to statistical analyses. In general, even without numerous numerical simulations, we can investigate the statistical properties of a stochastic process if the PDF of the random variable at any time is available by solving the corresponding Fokker-Planck equation. Fortunately, the PDF for the Bessel process is already known (Guarnieri et al., 2017). Thus, it should be possible to calculate some statistical properties of strong ground motion at low computational costs.

Acknowledgments

This work was supported by JSPS KAKENHI Grant (18K13637) and the Japan–Russia Research Cooperative Program (JSPS and RFBR, project No. J19–721). The author has no conflict of interest, financial or otherwise. No data were used in this study.

References

Abercrombie, R. E. (1995). Earthquake source scaling relationships from -1 to 5 M_L using seismograms recorded at 2.5-km depth. *Journal of Geophysical Research: Solid Earth*, *100*(B12), 24015–24036. doi: 10.1029/95jb02397

Andrews, D. J. (1980). Fault impedance and earthquake energy in the Fourier transform domain. *Bulletin of the Seismological Society of America*, *70*(5), 1683–1698.

Andrews, D. J. (1981). A stochastic fault model: 2. time-dependent case. *Journal of Geophysical Research: Solid Earth*, *86*(B11), 10821–10834. doi: 10.1029/jb086ib11p10821

Aso, N., Ando, R., & Ide, S. (2019). Ordinary and slow earthquakes reproduced in a simple continuum system with stochastic temporal stress fluctuations. *Geophysical Research Letters*, *46*(24), 14347–14357. doi: 10.1029/2019gl085010

Boatwright, J. (1980). A spectral theory for circular seismic sources; simple estimates of source dimension, dynamic stress drop, and radiated seismic energy. *Bulletin of the Seismological Society of America*, *70*(1), 1–27.

Göing-Jaeschke, A., & Yor, M. (2003). A survey and some generalizations of Bessel processes. *Bernoulli*, *9*(2). doi: 10.3150/bj/1068128980

Guarnieri, F., Moon, W., & Wettlaufer, J. S. (2017). Solution of the Fokker-Planck equation with a logarithmic potential and mixed eigenvalue spectrum. *Journal of Mathematical Physics*, *58*(9), 093301. doi: 10.1063/1.5000386

Hamana, Y., & Matsumoto, H. (2013). The probability distributions of the first hitting times of Bessel processes. *Transactions of the American Mathematical Society*, *365*(10), 5237–5257. doi: 10.1090/s0002-9947-2013-05799-6

Hirano, S., & Yagi, Y. (2017). Dependence of seismic and radiated energy on shorter wavelength components. *Geophysical Journal International*, *209*(3), 1585–1592. doi: 10.1093/gji/ggx108

Houston, H. (2001). Influence of depth, focal mechanism, and tectonic setting on the shape and duration of earthquake source time functions. *Journal of Geophysical Research: Solid Earth*, *106*(B6), 11137–11150. doi: 10.1029/2000jb900468

Ide, S. (2008). A Brownian walk model for slow earthquakes. *Geophysical Research Letters*, *35*(17). doi: 10.1029/2008gl034821

Kanamori, H. (2014). The diversity of large earthquakes and its implications for hazard mitigation. *Annual Review of Earth and Planetary Sciences*, *42*(1), 7–26. doi: 10.1146/annurev-earth-060313-055034

Madariaga, R., & Ruiz, S. (2016). Earthquake dynamics on circular faults: a review 1970–2015. *Journal of Seismology*, *20*(4), 1235–1252. doi: 10.1007/s10950-016-9590-8

Matthews, M., Ellsworth, W., & Reasenberg, P. (2002). A Brownian model for recurrent earthquakes. *Bulletin of the Seismological Society of America*, *92*(6), 2233–2250. doi: 10.1785/0120010267

Meier, M.-A., Heaton, T., & Clinton, J. (2016). Evidence for universal earthquake rupture initiation behavior. *Geophysical Research Letters*, *43*(15), 7991–7996. doi: 10.1002/2016gl070081

Mikumo, T. (2003). Stress-breakdown time and slip-weakening distance inferred from slip-velocity functions on earthquake faults. *Bulletin of the Seismological Society of America*, *93*(1), 264–282. doi: 10.1785/0120020082

Rößler, A. (2010). Runge–Kutta methods for the strong approximation of solutions of stochastic differential equations. *SIAM Journal on Numerical Analy-*

sis, *48*(3), 922–952. doi: 10.1137/09076636x

Uchide, T., & Ide, S. (2010). Scaling of earthquake rupture growth in the Parkfield area: Self-similar growth and suppression by the finite seismogenic layer. *Journal of Geophysical Research*, *115*(B11). doi: 10.1029/2009jb007122

Wu, T.-H., Chen, C.-C., Lovallo, M., & Telesca, L. (2019). Informational analysis of Langevin equation of friction in earthquake rupture processes. *Chaos: An Interdisciplinary Journal of Nonlinear Science*, *29*(10), 103120. doi: 10.1063/1.5092552

Yin, J., Li, Z., & Denolle, M. A. (2021). Source time function clustering reveals patterns in earthquake dynamics. *Seismological Research Letters*, *92*, 2343–2353. doi: 10.1785/0220200403